SLAC-PUB-9279
May 2002
A/E

Measurements of Accelerator-Produced Leakage Neutron and Photon Transmission through Concrete*

K. R. Kase, W. R. Nelson, A. Fasso, J. C. Liu, X. Mao,
T. M. Jenkins,and J. H. Kleck†

Stanford Linear Accelerator Center, Stanford University, Stanford, CA 94309

To be published in Health Physics

* Work supported by Department of Energy contract DE-AC03-76SF00515.
† Varian Corporation, Palo Alto, CA 94304.

Abstract

Optimum shielding of the radiation from particle accelerators requires knowledge of the attenuation characteristics of the shielding material. The most common material for shielding this radiation is concrete, which can be made using various materials of different densities as aggregates. These different concrete mixes can have very different attenuation characteristics. Information about the attenuation of leakage photons and neutrons in ordinary and heavy concrete is, however, very limited. To increase our knowledge and understanding of the radiation attenuation in concrete of various compositions, we have performed measurements of the transmission of leakage radiation, photons and neutrons, from a Varian Clinac 2100C medical linear accelerator operating at maximum electron energies of 6 and 18 MeV. We have also calculated, using Monte Carlo techniques, the leakage neutron spectra and its transmission through concrete. The results of these measurements and calculations extend the information currently available for designing shielding for medical electron accelerators. Photon transmission characteristics depend more on the manufacturer of the concrete than on the atomic composition. A possible cause for this effect is a non-uniform distribution of the high-density aggregate, typically iron, in the concrete matrix. Errors in estimated transmission of photons can exceed a factor of three, depending on barrier thickness, if attenuation in high-density concrete is simply scaled from that of normal density concrete. We found that neutron transmission through the high-density concretes can be estimated most reasonably and conservatively by using the linear tenth-value layer of normal concrete if specific values of the tenth-value layer of the high-density concrete are not known. The reason for this is that the neutron transmission depends primarily on the hydrogen content

of the concrete, which does not significantly depend on concrete density. Errors of factors of two to more than ten, depending on barrier thickness, in the estimated transmission of neutrons through high-density concrete can be made if the attenuation is scaled by density from normal concrete.

Introduction

Optimum shielding of the radiation from particle accelerators requires knowledge of the attenuation characteristics of the shielding material. The most common material for shielding this radiation is concrete because concrete is inexpensive and effective for shielding both photon and neutron radiation. Concrete can be made using various materials of different densities as aggregates. Consequently, different concrete mixes can have very different attenuation characteristics. Typically concrete mixtures consist of about 80 percent by weight of oxygen and silicon, with the rest of the composition comprising calcium, aluminum and lesser quantities of sodium, potassium and iron. Very important for neutron attenuation is hydrogen, which makes up less than one percent by weight of most concrete. The composition of an ordinary concrete, NBS 04, (Shultis and Faw 1996) with a density of 2.35 g cm^{-3} (about 147 lb ft^{-3}) is given in Table 1. However, "ordinary" concrete can have different compositions in practice, usually depending on the aggregate used. Often concrete is made with much higher density aggregates to increase its attenuation of photons and reduce the space needed for shielding. These high-density concretes can have very different compositions and densities depending on the manufacturer or provider.

Recently a number of companies have offered pre-cast concrete blocks for shielding construction. These blocks can provide advantages over concrete poured in place. In particular, they can assure a more uniform distribution of the aggregate and more uniform density. They also can eliminate the difficulties related to the transport and pouring of heavy concrete. Several publications contain information about shielding both photons and neutrons using concrete (Shultis and Faw, 1996; Patterson and Thomas, 1973, NCRP, 1977; IAEA, 1979). Shielding data, including half-value and tenth-value layers for concrete of various compositions from these and other sources are collected in the Handbook of Health Physics and Radiological Health, 3rd Edition (Shleien, Slaback and Birkey, 1998). However, these data are normally for ordinary concrete and given for primary photons and neutrons, not for leakage photons and neutrons. Maruyama, et al. (1971), Lokan, et al. (1972) and Barish (1993) have published primary photon transmission data for specific high-density concretes.

Information about the attenuation of leakage photons and neutrons in ordinary and heavy concrete is, however, very limited. To increase our knowledge and understanding of the attenuation of leakage radiation in concrete of various compositions, we have performed measurements of the transmission of leakage radiation, photons and neutrons, from a Varian Clinac 2100C (Varian Medical Systems, Palo Alto, CA) medical linear accelerator operating at maximum electron energies of 6 and 18 MeV. We have also calculated, using Monte Carlo techniques, the leakage neutron spectra and its transmission through concrete (Kase, K. R., et al., 1998; Liu, et al., 1997). The results of these measurements and calculations extend the information currently available for designing shielding for medical electron accelerators.

Materials and Methods

Measurements were made in a test cell (typically 7 m x 7 m x 4.75 m high) at Varian Associates using a standard Clinac 2100C linear electron accelerator. The accelerator was oriented to deliver the x-ray beam vertically at the ceiling of the test cell (Fig. 1). The detector housing was placed in line with the Linac target at 90º to the beam direction at a distance of 3 meters from the target. The detector housing was constructed of concrete, providing 60 cm of shielding on all sides except the side open to the accelerator. The cavity in which the detectors were placed was lined with lead and polyethylene to reduce the influence of unwanted scattered radiation further. Leakage photon radiation was measured with the accelerator operating at 6 and 18 MeV maximum electron energies. Measurements were made of leakage neutron radiation at the same point with the accelerator operating at 18 MeV.

Concrete of various densities was obtained from three manufacturers, A (Atomics International, Frederick, PA), E (New England Lead Burning, Woburn, MA) and S (Nuclear Shielding Supplies and Services, Tucson, AZ). The concrete compositions by weight percent are given in Table I, compared with the NBS 04 ordinary concrete (Shultis and Faw 1996). (Note that mnemonically A230, for example, identifies the manufacturer, A, and the density, 2.30 g cm^{-3}.) Core samples from each concrete slab were sent to an independent laboratory for analysis to determine the compositions. Densities of the various concretes were determined from the core samples and also by weighing and measuring the volume of each slab. The method of manufacture differed among the suppliers. Some of the high-density concrete contained large pieces of iron or steel. Others contained a mixture of sizes of iron from large pieces to powder mixed uniformly in the matrix. All of the concrete slabs provided were 7.6 or 15.2 cm thick and had lateral dimensions large enough to completely cover the side of the detector housing facing the accelerator (nominally 122 cm x 122 cm). The slabs ranged in weight from about 265 kg to about 1100 kg depending on thickness and density.

Measurements were made beginning with the detector housing open to the accelerator. Subsequent measurements were made through increasing thicknesses of the various commercially supplied concrete slabs of different densities. The maximum thickness of concrete used was 53 cm, so that first and second (and in some cases third) tenth value layers of the various concrete mixes were determined. The variable collimators on the accelerator were closed during the measurements.

To provide sufficient sensitivity for the lowest dose rates expected, the photon dose measurements were made using a 1500 cm^3 air ionization chamber (Keithley Instruments, Solon, OH). For the neutron measurements, indium foils approximately 4.5 cm in diameter and weighing 2.70 $\pm$0.02 g were used. These foils were placed in cylindrical polyethylene containers (Fig. 2) that were designed for measuring either the neutron fluence (cadmium covered) or dose equivalent (remmeter design). The irradiation times depended on the thickness of the attenuating concrete. Following exposure, the indium foils were allowed to decay for approximately 10 minutes. The gamma ray activity from the 54.2 minute ^{116}In was determined using a proportional counter for its high efficiency. Measured activity was corrected for decay to the time of irradiation and all values were normalized to the activity measured when there was no concrete between the source and detector.

Photon measurements were made with all seven samples of concrete. Neutron measurements were made using only the concrete slabs of three densities from a single manufacturer (A).

Mao, et al. (1997) calculated photoneutron production in the Clinac 2100/2300C accelerators using the EGS4 Monte Carlo code (Nelson, et al. 1985) and a photoneutron scoring method. Kase, et al. (1998) described the calculation of leakage neutron fluence and energy spectra in a typical accelerator room using a combination of the EGS4, EVAP4 (ORNL 1974) and MORSE (Emmett 1984) codes. Liu (1997) used the spectrum calculated for incident 22.3 MeV electrons (20 MV photon beam) as input in MCNP 4A (Briesmeister 1993) to calculate the dose equivalent transmission in ordinary density concrete (NBS 04) and two of the high-density concretes (A395 and A468).

Results and Discussion

Photons

Results of the photon transmission measurements are presented in Figs. 3 – 7 and Table II. The uncertainty in the measurement of density thickness for the concrete is about $\pm$4% based on the variation in density measured for the various samples. The statistical uncertainty in each photon dose measurement is about $\pm$2.5 % based on one standard deviation of repeated measurements. To determine the total uncertainty in the dose transmission the fractional uncertainty for the measurement through a given thickness was added in quadrature with the fractional uncertainty of the measurement taken with no attenuation. The uncertainty in the photon tenth-value layer (TVL) was determined by adding in quadrature the fractional uncertainties of the dose measurement with that of the concrete density thickness measurement. This uncertainty is about $\pm$5%.

For any individual concrete (Figs. 3 and 4) the log of relative dose as a function of density thickness was fitted by linear regression. If there were three or more data points covering each of the first and second decades, separate linear regressions were made to determine both first and second TVL. There is no indication that the first TVL is different from subsequent TVLs within the uncertainties for 6 MV photons. At 18 MV there is an indication that the second TVL is greater than the first TVL (Table II). Fig. 5 shows the values of the calculated TVLs as a function of concrete density. It might be expected that the TVLs for all the concretes would be approximately equivalent when expressed in the quantity density thickness (g cm^{-2}). For both 6 and 18 MV leakage photons the first ρTVL for all three concretes from manufacturer A and the 4.11 g cm^{-3} concrete from manufacturer S agree approximately within the uncertainties. The first ρTVL of the concretes from manufacturer E agree with each other at 6 and 18 MV and overlap the high-density concretes from manufacturer A at 6 MV. The TVL for the concrete from manufacturer S appears to scale better with density than do the TVLs of the other high-density concretes. At 6 MV the first and second ρTVLs of the S concretes agree within the uncertainties with those of the normal density concrete, A230. At 18 MV the scaling is not as good.

In Figs. 6 and 7 the transmission data for leakage photons through ordinary concrete (A230) from these measurements are compared with previously reported transmission of

6 MV and 18 MV – 25 MV primary and leakage photons through normal density concrete. In Fig. 6 calculations of leakage photons by Nelson and LaRiviere (1984), measurements of Karzmark and Capone (1968) of leakage radiation and transmission of primary photons given in NCRP Report No. 51 (1977) are compared. Fig. 7 shows the comparison of transmission of leakage 18 MV photons from this measurement and calculations of Nelson and LaRiviere for leakage 25 MV photons (1984), measurements of leakage 24 MV photons by LaRiviere (1984), and transmission of 18 MV primary radiation taken from NCRP Report No. 51 (1977).

The measured leakage data for 18 MV appear to be in reasonable agreement with the earlier calculations and measurements of leakage of 24 MV and 25 MV photons (Fig. 7). Nelson and LaRiviere (1984) calculated 83 g cm^{-2} and 74 g cm^{-2} for the first and second ρTVL, respectively, at 25 MV and LaRiviere (1984) measured 78 g cm^{-2} for the ρTVL at 24 MV. Values for the first ρTVL agree reasonably well with these measurements considering the uncertainties. The data for 6 MV from these measurements appear to fall below the calculations of Nelson and LaRiviere (1984), which seem to agree better with the primary radiation transmission reported in NCRP Report No. 51 (Fig. 6). Nelson and LaRiviere (1984) calculated 78 g cm^{-2} and 64 g cm^{-2} for the first and second ρTVL respectively at 6 MV.

Maruyama, et al. (1971), Lokan, et al. (1972) and Barish (1993) have published the results of measurements of primary photon transmission through various high-density concretes. Those results are not directly comparable with the measurements of leakage radiation reported here. However, they do give information about the variability of different concrete mixes and the approximate magnitude of the TVL. Maruyama reported TVL for normal concrete at a density of 2.26 g cm^{-2} and concrete with a density of 3.31 g cm^{-2}; Lokan measured transmission through concretes with densities of 2.88 g cm^{-2}, 3.87 g cm^{-2}, and 4.28 g cm^{-2}; Barish reported on measurements using concrete (Ledite) with a density of 4.71 g cm^{-2}. First ρTVLs for 5 – 6 MV photons ranged from 71 – 79 g cm^{-2}. Second ρTVLs reported by Lokan were in the same range. At 16 – 20 MV the first ρTVLs ranged from 85 – 107 g cm^{-2} with the higher values generally associated with the lower density concretes. The second ρTVLs were again in the same range.

Neutrons

Results of the neutron transmission measurements through the three concretes of different densities provided by manufacturer A are shown in Figs. 8 and 9 and Table II. Linear regression fits to the data were made as described above to determine first and second TVLs, and are shown in the figures. The uncertainties in the concrete density thickness are the same as described above. The statistical uncertainties in the neutron fluence and dose equivalent rate are determined from the counting statistics of the indium foils. Based on one standard deviation of the counts these were 5.5 % for the A230, 8 % for the A395 and 1 % for the A468 concrete. The total uncertainties for the transmission measurements and the TVLs were determined as described above. Within the uncertainties the dose equivalent and fluence TVLs agree. There appears to be no significant difference between the first and second TVL for leakage neutrons. This indicates that the neutron energy spectrum does not change significantly as the neutrons penetrate the concrete.

However, it is clear that for neutrons the TVLs, expressed in density thickness, of concretes of various densities increase with density.

Barish (1993) has reported a ρTVL equal to 136 g cm^{-2} in Ledite (4.71 g cm^{-3}) for direct neutrons produced at 16 MV and not moderated by transmission through the accelerator head shielding. This result is to be compared with the result given in NCRP Report No. 51 (1977) discussed below, for which the ρTVL in normal concrete is 57 g cm^{-2}.

Fig. 10 compares the neutron transmission data from these measurements and the transmission calculated using the methodology described in NCRP Report No. 79 (1984). Also shown is the transmission of neutrons generated by 16 MeV electrons on a Pt target that is taken from NCRP Report No. 51 (1977). The methodology described in NCRP Report No 79 represents the measured transmission data quite well (especially the slope of the transmission curve). The transmission data taken from Report No. 51 is for neutrons directly from a bare target that have not passed through the typical medical accelerator head shielding. Those neutrons clearly have a higher mean energy than the leakage neutrons measured in this study.

The calculated neutron transmission, shown in Fig. 11, agrees reasonably well with the measured transmission shown in Fig. 9. The first and second TVLs for the A395 and A468 concretes are 16.5 cm and 17.0 cm respectively from the calculated transmission. The first and second TVLs from the measured data for 18 MV leakage neutrons are 16 cm. There is a disagreement of about $\pm$2 cm for the normal density concrete, but the density and composition of the A230 concrete used in the measurement was somewhat different from that of the NBS 04 concrete used in the calculation (see Table I). This result indicates that the calculated neutron spectrum (Kase, et al. 1998) and the MCNP 4A code are adequate to estimate neutron transmission through barrier materials. Thus, further transmission calculations can be made for barrier designs incorporating, for example, concrete and steel or lead.

Conclusions

The results of this investigation have provided new information about the transmission of leakage photons and neutrons through concrete, especially high-density mixes.

Photons

Photon transmission characteristics depend more on the manufacturer of the concrete than on the atomic composition. Scaling the photon transmission from normal density concrete to the concrete with the highest Fe content based on atomic composition would indicate an expected decrease in TVL of 2% to 3% when expressed as density thickness, i.e. ρTVL. In fact, differences of more than 20% were measured, and in most cases the TVL increased with increasing iron content. A possible cause for this effect is a non-uniform distribution of the high-density aggregate, typically iron, in the concrete matrix. If the iron is present as relatively large pieces, there are transmission paths for photons that can avoid some of the the high-density material. Errors in estimated transmission of photons can exceed a factor of three, depending on barrier thickness, if attenuation in high-density concrete is simply scaled from that of normal density concrete.

Neutrons

We have shown that results using the method for determining neutron transmission through ordinary concrete that is described in NCRP Report No. 79 (1984) agree well with our measurements, and are somewhat (~20 percent) conservative. Transmission calculations made using Monte Carlo methods and calculated neutron leakage spectra give results that are comparable with the measurements.

It is clear that neutron transmission through the high-density concretes can be estimated most reasonably and conservatively by using the linear tenth-value thickness of normal concrete if specific values of the tenth-value thickness of the high-density concrete are not known. The reason for this is that the neutron transmission depends primarily on the hydrogen content of the concrete, which does not significantly depend on concrete density. Errors of factors of two to more than ten, depending on barrier thickness, in the estimated transmission of neutrons through high-density concrete can be made if the attenuation is scaled by density from normal concrete.

Finally, because the leakage neutron energy spectrum is independent of position outside the direct radiation beam, the TVL for leakage neutrons will not vary with angle measured relative to the direct beam (Elsalim 1994; Kase, et al. 1998).

References

Barish RJ. Evaluation of a new high-density shielding material. Health Phys 64:412-416; 1993.

Briesmeister JF (ed). MCNP – A general Monte Carlo n-particle transport code. Version 4A. Los Alamos: Los Alamos National Laboratory; LA-12625-M; 1993.

Elsalim MM. Characterization of the neutron environment around Varian medical accelerators. San Jose, CA: San Jose State University; Thesis; 1994.

Emmett MB. The MORSE Monte Carlo radiation transport code system. Oak Ridge: Oak Ridge National Laboratory; ORNL-4972; 1984.

International Atomic Energy Agency. Radiological safety aspects of the operation of electron linear accelerators. Vienna: International Atomic Energy Agency; Technical Report Series No. 188; 1979.

Karzmark CJ, Capone T. Measurements of 6 MV x rays, Part III. Characteristics of secondary radiation. Brit J Radiol 41:227-230; 1968.

Kase KR, Mao XS, Nelson WR, Liu JC, Kleck JH, Elsalim, M. Neutron fluence and energy spectra around the Varian Clinac 2100C/2300C medical accelerator. Health Phys 74:38-47; 1998.

LaRiviere PD. Transmission in concrete of primary and leakage x rays from a 24-MV medical linear accelerator. Health Phys 47:819-827; 1984.

Liu JC, Kase KR, Mao XS, Nelson WR, Kleck JH, Johnson S.

Calculations of photoneutrons from Varian accelerators and their transmissions in materials. Stanford: Stanford Linear Accelerator Center;. SLAC-PUB-7404; 1997.

Lokan KH, Sherman NK, Gellie RW, Henry WH, Lévesque R, Nowack A, Teather GG, Lundquist JR. Bremsstrahlung attenuation measurements in ilmenite loaded concretes. Health Phys 23:193-199; 1972.

Mao XS, Kase KR, Liu JC, Nelson WR, Kleck JH, Johnson S. Neutron sources in the Varian Clinac 2100C/2300C medical accelerator calculated by the EGS4 code. Health Phys 72:524-529; 1997.

Maruyama T, Kumamoto Y, Kato Y, Hashizume T, Yamamoto M. Attenuation of 4-32 MV x-rays in ordinary concrete, heavy concrete, iron and lead. Health Phys 20:277-284; 1971.

Nelson WR, LaRiviere PD. Primary and leakage radiation calculations at 6, 10, and 25 MeV. Health Phys 47:811-818; 1984.

Nelson WR, Hirayama H, Rogers, DWO. The EGS4 code system. Stanford: Stanford Linear Accelerator Center; SLAC-265; 1985.

National Council on Radiation Protection and Measurements. Radiation protection design guidelines for 0.1 – 100 MeV particle accelerator facilities. Bethesda: National Council on Radiation Protection and Measurements; NCRP Report No. 51; 1977.

National Council on Radiation Protection and Measurements. Neutron contamination from medical accelerators. Bethesda: National Council on Radiation Protection and Measurements; NCRP Report No. 79; 1984.

ORNL. The EVAP calculation of particle evaporation from excited compound nuclei.

Oak Ridge: Oak Ridge National Laboratory; PSR-10; 1974.

Patterson, HW, Thomas, RH Accelerator health physics. New York: Academic Press; 1973.

Shleien, B, Slaback, LA, Birkey, BK. Handbook of health physics and radiological health. 3rd ed. Baltimore: Williams and Wilkins; 1998.

Shultis, JK, Faw, RE. Radiation shielding. Upper Saddle River: Prentice Hall PTR; 1996.

Table I Concrete Composition

	NBS 04	A230	E391	A395	S411	A468	S471	E480
H	0.55%	0.61%	0.70%	0.50%	0.50%	0.89%	0.50%	0.50%
C	0.00%	5.48%	0.55%	0.50%	0.50%	0.55%	0.50%	0.79%
O	49.57%	51.02%	50.51%	35.17%	34.31%	37.07%	32.89%	14.52%
Na	1.70%	0.11%	0.18%	0.05%	0.06%	0.14%	0.08%	0.09%
K	1.91%	0.21%	0.10%	0.11%	0.05%	0.12%	0.05%	0.09%
Mg	0.26%	4.35%	1.27%	0.20%	0.12%	0.36%	0.16%	0.17%
Al	4.55%	0.70%	1.49%	0.56%	0.38%	0.80%	0.49%	0.42%
Si	31.36%	20.26%	4.20%	1.47%	1.87%	2.45%	2.19%	1.88%
S	0.13%	0.26%	0.76%	0.20%	0.10%	0.29%	0.11%	0.26%
Ca	8.26%	16.02%	16.34%	5.09%	4.80%	9.98%	7.08%	6.20%
Fe	1.23%	0.98%	23.90%	56.15%	57.31%	47.35%	55.95%	75.08%

Table II Tenth Value Layers for Leakage Radiation

($g\ cm^{-2}$)

	A230	E391	A395	S411	A468	S471	E480
6 MV Photons							
ρTVL1 ($g\ cm^{-2}$)	63±3	78±4	73±4	63±3	68±3	59±3	74±4
TVL1 (cm)	27±1	20±1	18±1	16±1	15±1	13±1	15±1
ρTVL2 ($g\ cm^{-2}$)	66±3	-	-	70±4	73±4	63±3	80±4
TVL2 (cm)	29±1	-	-	17±1	16±1	13±1	17±1
18 MV photons							
ρ TVL1 ($g\ cm^{-2}$)	89±4	112±6	96±5	96±5	100±5	79±4	111±6
TVL1 (cm)	40±2	29±1	24±1	24±1	21±1	17±1	23±1
ρTVL2 ($g\ cm^{-2}$)	98±5	-	117±6	111±6	118±6	116±6	123±6
TVL2 (cm)	43±2	-	30±2	27±1	25±1	25±1	26±1
Neutrons							
(Dose Equivalent)							
ρTVL1 ($g\ cm^{-2}$)	41±3	-	60±5	-	76±3	-	-
TVL1 (cm)	19±1	-	16±1	-	16±1	-	-
TVL1 (cm) Calculated	17	-	17	-	17	-	-
ρTVL2 ($g\ cm^{-2}$)	45±3	-	63±6	-	75±3	-	-
TVL2 (cm)	20±1	-	16±1	-	16±1	-	-
TVL2 (cm) Calculated	23	-	17	-	17	-	-

Figure Captions

Fig. 1 Line drawing of the experimental set up showing the accelerator and the shielded detector housing. The concrete slabs were 15 cm (6 inch) thick high density concrete. The detector chamber was lined with 2.54 cm (1 inch) thick lead and flexible borated silica. The slabs shown above and below the chamber were polyethylene.

Fig. 2 Photograph of the neutron detectors. Indium foils were placed in cylindrical polyethylene containers that were designed for measuring either the neutron fluence (white) or dose equivalent (black).

Fig. 3 Measured transmission of leakage photons from a Clinac 2100C operating at 6 MV through concretes of various densities from three manufacturers (A, E, and S).

Fig. 4 Measured transmission of leakage photons from a Clinac 2100C operating at 18 MV through concretes of various densities from three manufacturers (A, E, and S).

Fig. 5 Measured photon first and second Tenth Value Layers as a function of concrete density. The uncertainties shown are $\pm 1\sigma$ based on the TVL measurement. The lines are linear fits to the data.

Fig. 6 Comparison of 6 MV photon transmission through normal concrete. Measurements reported here for A230 concrete are compared with leakage photon calculations of Nelson and LaRiviere (1984) [Ne}, measurement of Karzmark and Capone of TVL for leakage radiation (1968) [Ka]; and transmission of 6 MV primary radiation taken from NCRP Report No. 51 (1977) [NCRP].

Fig. 7 Comparison of 18 - 24 MV leakage photon transmission through normal concrete. Measurements reported here for 18 MV leakage photons through A230 concrete are compared with calculations of Nelson and LaRiviere (1984) for 25 MV leakage [Ne], measurements of LaRiviere (1984) for 24 MV leakage [La], and transmission of 18 MV primary radiation taken from NCRP Report No. 51 (1977) [NCRP].

Fig. 8 Measured transmission of leakage neutron fluence from a Clinac 2100C operating at 18 MV through concrete provided by manufacturer A. Lines are regression fits to the data.

Fig. 9 Measured transmission of leakage neutron dose equivalent from a Clinac 2100C operating at 18 MV through concrete provided by manufacturer A. Lines are regression fits to the data.

Fig. 10 Comparison of neutron dose equivalent transmission through normal concrete. Measurements reported here for A230 concrete are compared with calculations based on the method described in NCRP Report No. 79 and with the transmission of neutrons generated by 16 MeV electrons on a platinum target taken from NCRP Report No. 51 (1977).

Fig. 11 Calculated relative transmission of leakage neutron dose equivalent through concrete for 22.3 MeV electrons incident on a tungsten/copper target.

Acknowledgements

This work was supported by Department of Energy Contract DE-AC03-76SF00515. The authors express their appreciation to R. C. McCall for his insights to the interpretation of the measured data.

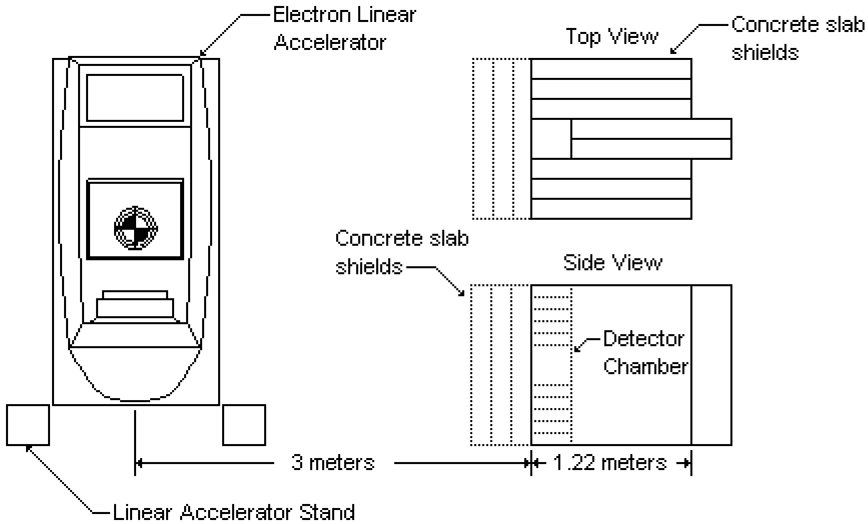
Electron Linear Accelerator
Top View
Concrete slab shields
Concrete slab shields
Side View
Detector Chamber
3 meters
1.22 meters
Linear Accelerator Stand

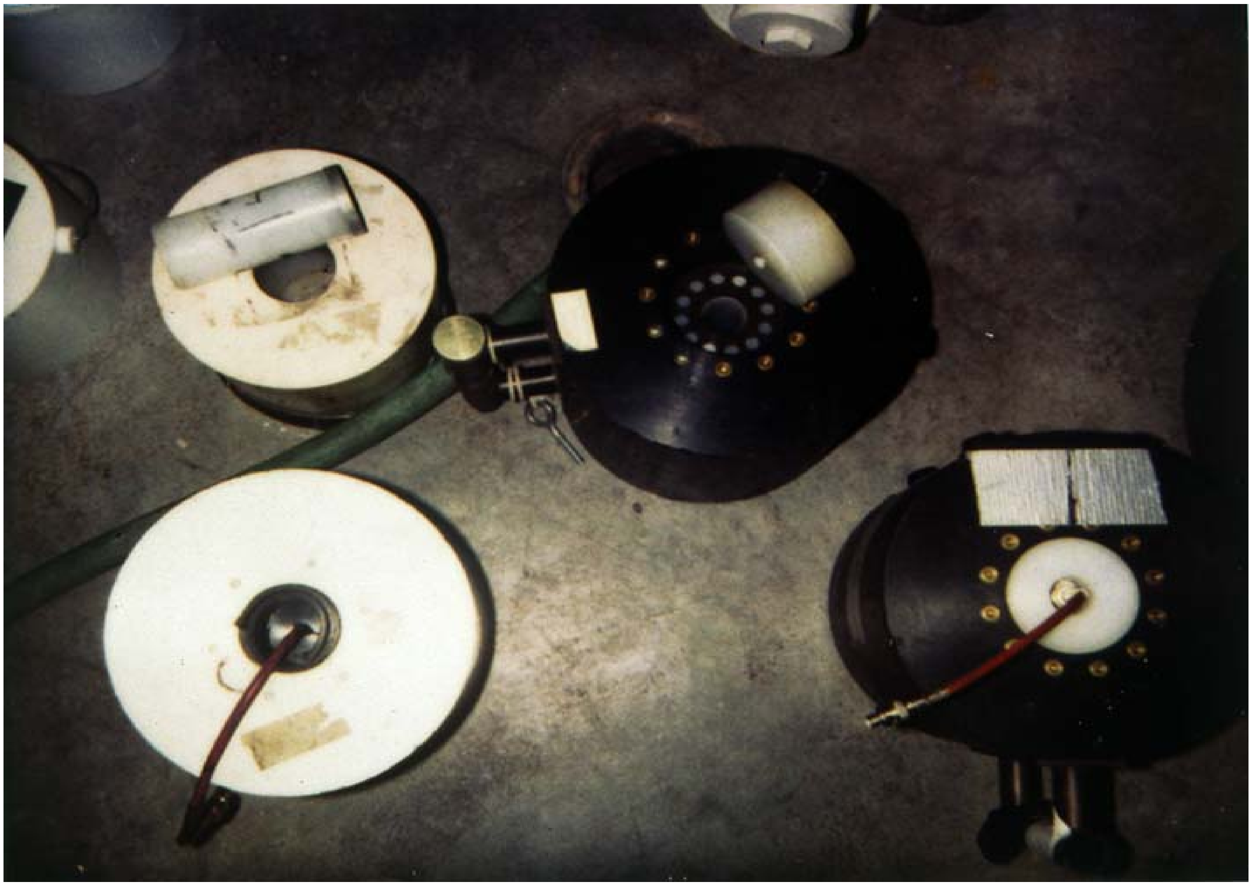

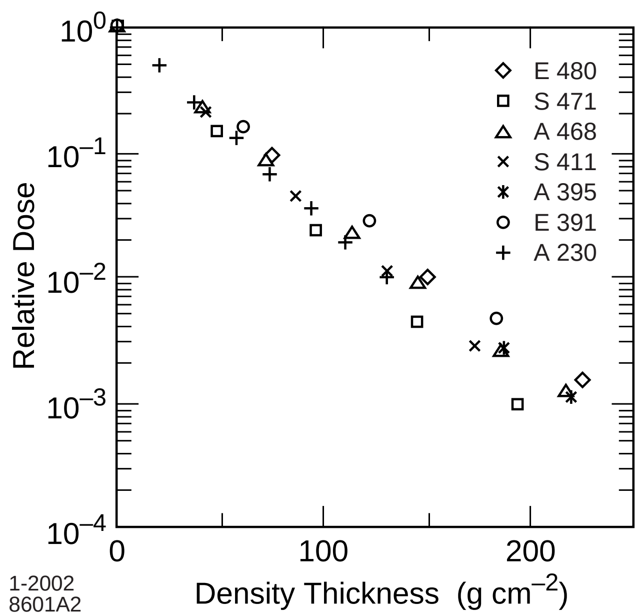

10^0
10^–1
10^–2
10^–3
10^–4
0
100
200
Relative Dose
Density Thickness (g cm^–2)
E 480
S 471
A 468
S 411
A 395
E 391
A 230
1-2002
8601A2

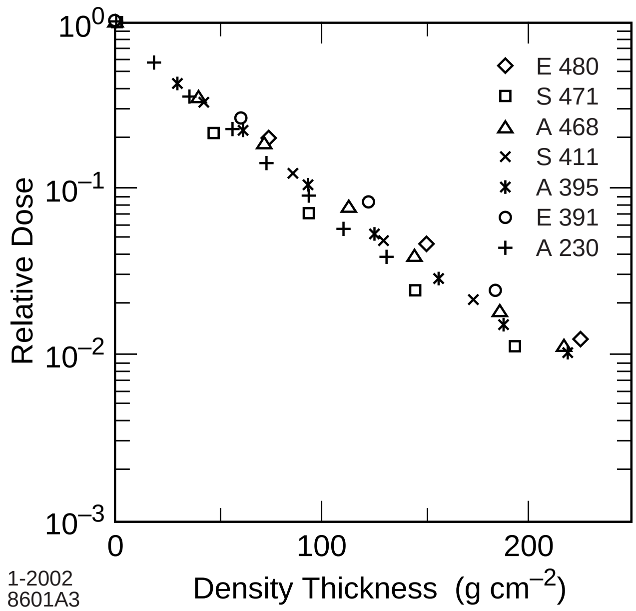

Relative Dose
Density Thickness (g cm^{-2})
10^{0}
10^{-1}
10^{-2}
10^{-3}
0
100
200
E 480
S 471
A 468
S 411
A 395
E 391
A 230
1-2002
8601A3

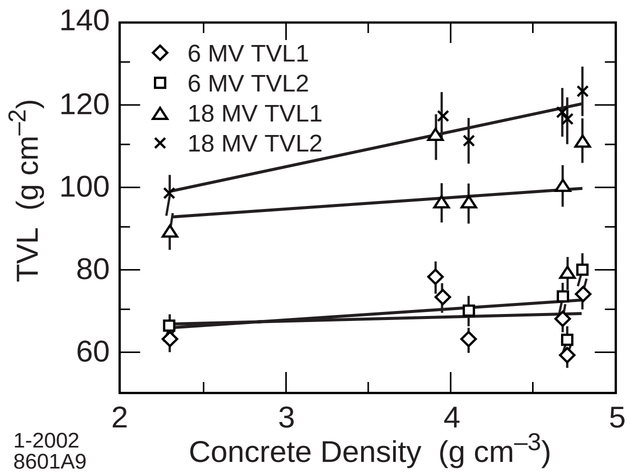

140
120
100
80
60
TVL (g cm^{-2})
6 MV TVL1
6 MV TVL2
18 MV TVL1
18 MV TVL2
2
3
4
5
Concrete Density (g cm^{-3})
1-2002
8601A9

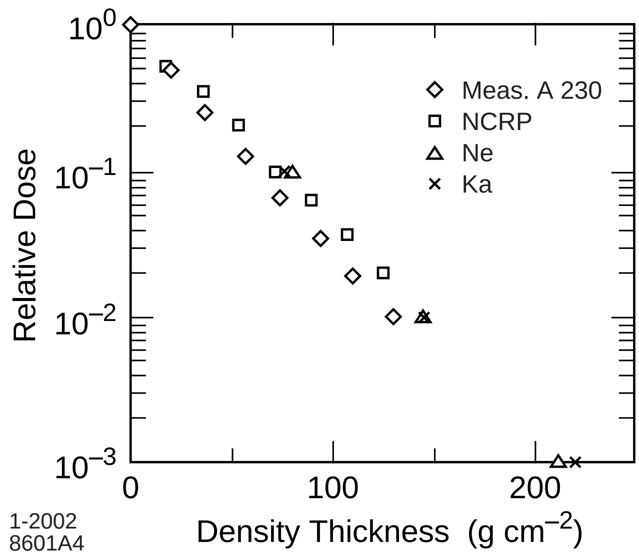

Relative Dose
10^0
10^{-1}
10^{-2}
10^{-3}
0
100
200
Density Thickness (g cm^{-2})
Meas. A 230
NCRP
Ne
Ka
1-2002
8601A4

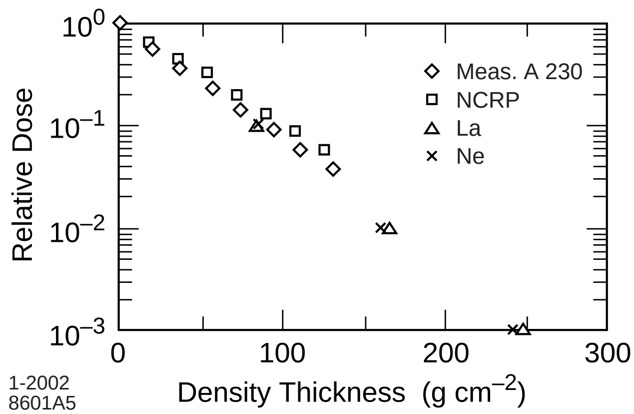

Relative Dose
10^0
10^–1
10^–2
10^–3
0
100
200
300
Density Thickness (g cm^–2)
Meas. A 230
NCRP
La
Ne
1-2002
8601A5

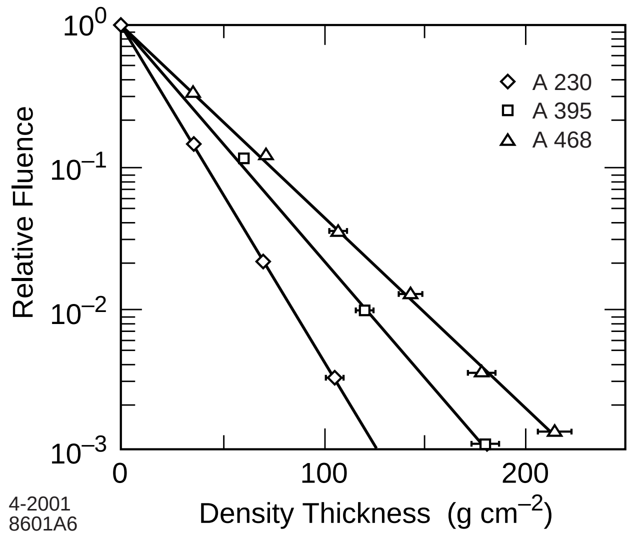

10^0
10^–1
10^–2
10^–3
Relative Fluence
A 230
A 395
A 468
0
100
200
Density Thickness (g cm^–2)
4-2001
8601A6

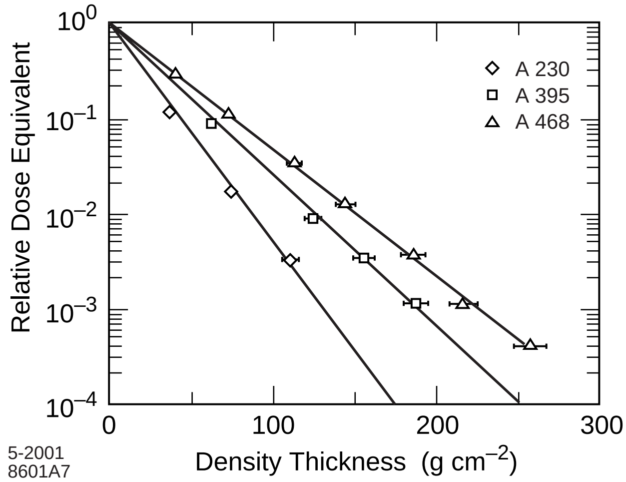

Relative Dose Equivalent
10^0
10^{-1}
10^{-2}
10^{-3}
10^{-4}
0
100
200
300
Density Thickness (g cm^{-2})
A 230
A 395
A 468
5-2001
8601A7

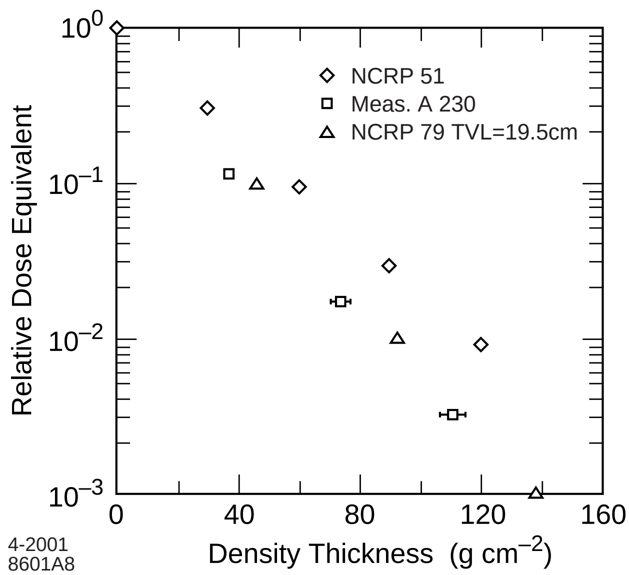

10^0
10^−1
10^−2
10^−3
Relative Dose Equivalent
NCRP 51
Meas. A 230
NCRP 79 TVL=19.5cm
0
40
80
120
160
Density Thickness (g cm^−2)
4-2001
8601A8

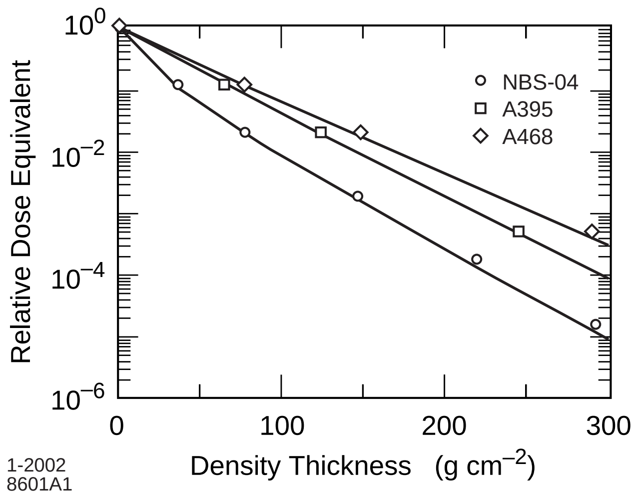

NBS-04
A395
A468
Relative Dose Equivalent
10^0
10^−2
10^−4
10^−6
0
100
200
300
Density Thickness (g cm^−2)
1-2002
8601A1